EPR, ^1H, and ^{13}C ENDOR Studies of a Quintet-State ^{13}C-Labeled Galvinoxyl-Type Tetraradical

Burkhard Kirste,* Michael Grimm, and Harry Kurreck*

Contribution from the Institut für Organische Chemie, Freie Universität Berlin, 1000 Berlin 33, West Germany. *Received April 25, 1988*

Abstract: The syntheses of unlabeled and fourfold ^{13}C-labeled tetraphenylmethane tetrakisgalvinols are described. Different paramagnetic species, i.e., a doublet-state monoradical, a triplet-state biradical, a quartet-state triradical, and a quintet-state tetraradical, can be generated by selective oxidation and identified by EPR, ^1H, and ^{13}C ENDOR spectroscopy. The zero-field splitting parameter D is about 1.1 mT for the biradical, but it is vanishingly small for the tetraradical because of its tetrahedral symmetry. An estimate of $J \approx 600$ MHz has been obtained for the scalar electron exchange interaction in the multispin systems.

Organic oligoradicals or multispin systems are characterized by scalar exchange interaction and dipolar coupling of the unpaired electrons in addition to Zeeman splitting and hyperfine interactions. These phenomena have been studied extensively in the case of biradicals and less often in triradicals[1-3] by EPR[4,5] and ENDOR (electron nuclear double resonance[6,7]) spectroscopy. Because of an increasing number of hyperfine components, the resolution of fluid-solution EPR spectra of oligoradicals deteriorates progressively for higher electron spin states (bi-, tri-, and tetraradicals). Moreover, relaxation caused by the electron–electron dipolar interaction (zero-field splitting) or modulation of the exchange interaction gives rise to line broadening. The higher resolution of ENDOR spectroscopy allows the determination of hyperfine couplings even in quartet-state triradicals[8] and quintet-state tetraradicals,[9] but the experiments are more difficult to perform than with monoradicals because of the unfavorable relaxation properties of these systems.

As has been demonstrated for bi-[10] and triradicals,[11] use of ^{13}C-labeled compounds offers two advantages. First, the (presumably) large ^{13}C hyperfine coupling may give rise to a resolved hyperfine structure in the EPR spectra even of tetraradicals, allowing a selective field setting in ENDOR experiments. Thus, different chemical species (e.g., mono-, bi-, or triradicals also present in the sample), isotopomers, or different electron spin states can be studied separately. Second, observation of ^{13}C ENDOR signals supplies additional evidence for the identity of the spin system under study.[10,11]

Here we report on the investigation of unlabeled **1d** and fourfold ^{13}C-labeled tetraphenylmethane tetrakisgalvinoxyls **2d**. The tetraradical was chosen to have (approximately) tetrahedral symmetry, since in this case the formation of a quintet state may be expected because all pairwise electron exchange interactions are equal. Moreover, the zero-field splitting and hence the disturbing influence of electron–electron dipolar relaxation would vanish.[9] Actually, a spectroscopic investigation of a tetrakisgalvinoxyl of lower symmetry was not successful: fluid-solution

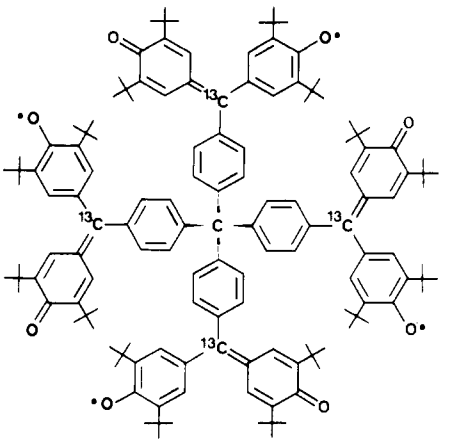

2d

and solid-state EPR spectra were not interpretable, and decent ENDOR signals of the tetraradical could not be detected.[12] Although the synthesis of an (unlabeled) approximately tetrahedral tetrakisgalvinol, derived from tetraphenylsilane, has been described previously,[9] the task of preparing a fourfold ^{13}C-labeled compound proved to be much more difficult.[13,14] In the present paper strategies for the synthesis of unlabeled and labeled tetraphenylmethane tetrakisgalvinols are discussed, and a detailed report on the spectroscopic properties of the mono-, bi-, tri-, and tetraradicals generated from these precursors is given. Short communications of these studies have already been published elsewhere.[13,15]

Results and Discussion

Synthesis. Since galvinols can be prepared from appropriate esters via a well-established organometallic pathway,[16] the tetraester **3** can be regarded as a suitable precursor for the synthesis of the tetrakisgalvinol **2**. A retrosynthetic analysis reveals that several pathways leading to **3** should be considered (Scheme I). Since the synthesis of a similar (unlabeled) tetraester, with silicon instead of carbon in the central position, has already been described,[9] the corresponding pathway shall be discussed first: **13** → **8** → **6** → **4** → **3**. However, tetrahalomethanes **13** are known to react with organometallic compounds quite differently from $SiCl_4$, i.e., carbenoid reactions take place whereas the formation of tetraphenylmethane has not been observed.[17] Although

(1) Hudson, A.; Luckhurst, G. R. *Mol. Phys.* **1967**, *13*, 409.
(2) Nowak, C.; Kothe, G.; Zimmermann, H. *Ber. Bunsenges. Phys. Chem.* **1974**, *78*, 265.
(3) Brickmann, J.; Kothe, G. *J. Chem. Phys.* **1973**, *59*, 2807.
(4) Scheffler, K.; Stegmann, H. B. *Elektronenspinresonanz*; Springer-Verlag: Berlin, 1970, Chapter D.
(5) Atherton, N. M. *Electron Spin Resonance*; Ellis Horwood: Chichester, 1973; Chapter 5.
(6) Kurreck, H.; Kirste, B.; Lubitz, W. *Angew. Chem.* **1984**, *96*, 171; *Angew. Chem., Int. Ed. Engl.* **1984**, *23*, 173.
(7) Kurreck, H.; Kirste, B.; Lubitz, W. *Electron Nuclear Double Resonance Spectroscopy of Radicals in Solution*; VCH Publishers: New York, 1988; Chapter 8.
(8) Kirste, B.; van Willigen, H.; Kurreck, H.; Möbius, K.; Plato, M.; Biehl, R. *J. Am. Chem. Soc.* **1978**, *100*, 7505.
(9) Kirste, B.; Harrer, W.; Kurreck, H. *Angew. Chem.* **1981**, *93*, 912; *Angew. Chem., Int. Ed. Engl.* **1981**, *20*, 873.
(10) Kirste, B.; Kurreck, H.; Schuberi, K. *Tetrahedron Lett.* **1978**, 777.
(11) Schuberi, K.; Kirste, B.; Kurreck, H. *Angew. Chem.* **1983**, *95*, 149; *Angew. Chem. Suppl.* **1983**, 128; *Angew. Chem., Int. Ed. Engl.* **1983**, *22*, 150.
(12) Gierke, W. Ph.D. Thesis, Freie Universität Berlin, 1978. Gierke, W.; Kirste, B.; Kurreck, H., unpublished results.
(13) Grimm, M.; Kirsie, B.; Kurreck, H. *Angew. Chem.* **1986**, *98*, 1095; *Angew. Chem., Int. Ed. Engl.* **1986**, *25*, 1097.
(14) Grimm, M. Ph.D. Thesis, Freie Universität Berlin, 1987.
(15) Kirsie, B.; Grimm, M.; Kurreck, H. *Proc. Congr. Ampere* **1986**, *23*, 470.
(16) Harrer, W.; Kurreck, H.; Reusch, J.; Gierke, W. *Tetrahedron* **1975**, *31*, 625.

0002-7863/89/1511-0108$01.50/0

Scheme I. Retrosynthetic Analysis[a]

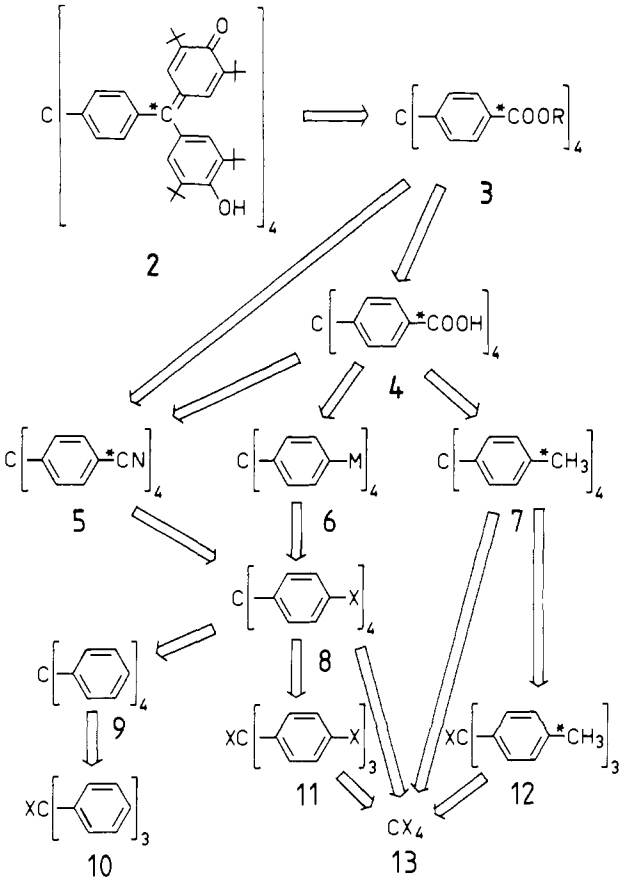

[a] The asterisks denote the ^{13}C-labeled positions: M, metal; X, halogen. Note that the ^{13}C-labeled tetrakisgalvinol is numbered **2**, whereas the respective unlabeled compound (not explicitly shown) is numbered **1**; radicals generated from **1** and **2** are designated by **a–d** (mono- to tetraradical).

tris(4-bromophenyl)chloromethane (**11**) can be prepared, e.g., by Friedel–Crafts alkylation of tetrachloromethane in moderate yield,[18] the feasibility of the conversion to **8** by a Grignard–Wurtz reaction[19] is questionable. More promising is the synthesis of the key compound **8** by bromination of tetraphenylmethane (**9**), which can be obtained from **10**.[20]

Tetracarboxylic acid **4** would be accessible from the tetrabromo compound **8** via **6** by fourfold metalation followed by reaction with carbon dioxide.[9] However, this pathway is not suitable for the preparation of the ^{13}C-labeled compound, since a large excess of $^{13}CO_2$ would be required. Alternatively, **4** might be obtained by oxidation of tetratolylmethane (**7**). Although **7** can be prepared in moderate yield via **12** by Friedel–Crafts alkylation of toluene followed by Grignard–Wurtz coupling with 4-methylphenylmagnesium bromide,[19] ^{13}C labeling is clearly not practicable by this method. More promising with respect to ^{13}C labeling is presumably the pathway via tetrahalo compound **8** and Wurtz–Fittig reaction, Grignard–Wurtz reaction, reaction with methyllithium, or reaction with a (mixed) lithium diorganocuprate(I).[21] However, these methods were not investigated in detail because various attempts to oxidize **7** did not give **4** in acceptable yield; at best, oxidation with CrO_3[22] yielded about 15% of **4**.[14]

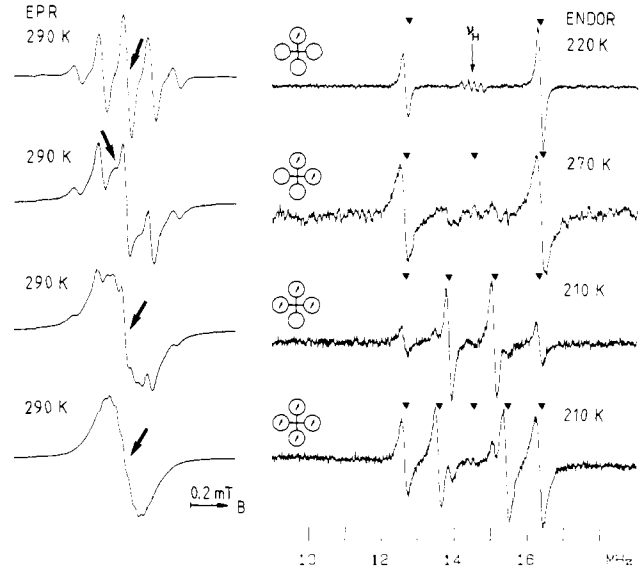

Figure 1. EPR (left) and ENDOR spectra (right) of different paramagnetic oxidation steps of unlabeled tetrakisgalvinol **1** in toluene. From top to bottom: monoradical **1a**, biradical **1b**, triradical **1c**, and tetraradical **1d**. The arrows in the EPR spectra indicate the field settings in the ENDOR experiments. The calculated ^1H ENDOR signal positions (galvinoxyl ring protons) are labeled by triangles (▼). Note that the EPR spectra of **1b** and **1c** exhibit contributions from other oxidation steps, see text.

A third method for the preparation of **4** involves tetranitrile **5**. Neither a Sandmeyer reaction nor a Rosenmund–von Braun reaction of **8** with copper(I) cyanide is likely to produce **5** in high yield, but the reaction of bromobenzene with potassium cyanide with palladium(II) acetate as catalyst is known to proceed quantitatively.[23] The tetranitrile **5** may then be converted to the tetraester **3** either by alcoholysis or by hydrolysis to **4** and subsequent esterification.

Unlabeled **1** and ^{13}C-labeled **2** tetrakisgalvinols were actually prepared according to pathway **10** → **9** → **8** → **5** → **4** → **3** → **2** (or **1**, respectively).[13,14] This sequence offers the advantage that the expensive ^{13}C-potassium cyanide is used as late as two steps before the final one. Tetraphenylmethane (**9**), prepared by Friedel–Crafts alkylation of aniline with triphenylcarbinol (**10**, X = OH), diazotization, and deamination,[20] was reacted with pure bromine to yield **8** (X = Br). Conversion of **8** to tetranitrile **5** was achieved with (99% ^{13}C-enriched) potassium cyanide in the presence of palladium(II) acetate.[23] Tetracarboxylic acid **4** was obtained by alkaline hydrolysis of **5** and converted to tetraester **3** with diazomethane. A drawback of the previously published galvinol synthesis[16] is that the organometallic reagent (2,6-di-*tert*-butyl-4-lithiophenoxy)trimethylsilane, prepared from (4-bromo-2,6-di-*tert*-butylphenoxy)trimethylsilane with *n*-butyllithium and 1,2-bis(dimethylamino)ethane, is not stable under the reaction conditions, thus limiting the yield. A substantial improvement of this step could be achieved by performing the metalation with *tert*-butyllithium at low temperature, and **2** was obtained from **3** in 94.5% yield. Since a high degree of isotopic labeling was required for the spectroscopic studies, highly ^{13}C-enriched (99%) potassium cyanide had to be employed (yielding 96% of [$^{13}C_4$]).

EPR and ENDOR of 1a–d, Fluid Solution. EPR spectra of the four paramagnetic oxidation steps **1a–d** generated from unlabeled tetrakisgalvinol **1** are depicted in Figure 1 (left). The EPR spectrum of **1a** exhibits the typical quintet hyperfine pattern of a galvinoxyl monoradical due to four galvinoxyl ring protons (a_H = 0.135 mT = 3.78 MHz). The resolution of the EPR spectra of the higher spin states (**1b–d**) is drastically decreased. Provided the electron exchange interaction is large ($|J| \gg |a|$), hyperfine

(17) Wittig, G.; Witt, H. *Ber. Dt. Chem. Ges.* **1941**, *74*, 1474.
(18) Gomberg, M.; Cone, L. H. *Ber. Dt. Chem. Ges.* **1906**, *39*, 1461, 3274. von Baeyer, A. *Ber. Dt. Chem. Ges.* **1907**, *40*, 3083.
(19) Schoepfle, C. S.; Trepp, S. G. *J. Am. Chem. Soc.* **1936**, *58*, 791.
(20) Neugebauer, F. A.; Fischer, H.; Bernhardi, R. *Chem. Ber.* **1976**, *109*, 2389.
(21) Posner, G. H. *Org. React.* **1975**, *22*, 253.
(22) Hopff, H.; Deuber, J. M.; Gallegra, P.; Said, A. *Helv. Chim. Acta* **1971**, *54*, 117.
(23) Takagi, K.; Okamoto, T.; Sakakibara, Y.; Ohno, A.; Oka, S.; Hayama, N. *Bull. Chem. Soc. Jpn.* **1975**, *48*, 3298.

interaction of the unpaired electrons with all contributing galvinoxyl ring protons (8, 12, or 16) should give rise to a respective increase in the number of hyperfine components ($n + 1$, binomial intensity ratio). Since the hyperfine splittings a^S are decreased relative to those of the monoradical (a^d),[8,9]

$$a^S = a^d/(2S) \quad (1)$$

where S is the electron spin quantum number, the resolution deteriorates progressively because the line widths are not reduced to the same extent. The line widths of the bi- and triradicals are even increased due to relaxation processes caused by the electron–electron dipolar interaction. Moreover, solutions of pure bi- or triradicals cannot be generated here because redox equilibria inevitably give rise to some extent of disproportionation. Another complication arises if the electron exchange interaction, though larger than the hyperfine interaction, is smaller than the thermal energy (kT) as may be assumed for the radicals under study.[24] In this case different spin states are present, i.e., a triplet and a singlet state (**1b**), a quartet and two doublet states (**1c**), and a quintet, three triplet, and two singlet states (**1d**). Since the respective doublet (**1c**) and triplet (**1d**) states are also paramagnetic, they should contribute to the EPR absorption, giving rise to a complicated hyperfine pattern.[1] The biradical spectrum (**1b**) is actually dominated by the monoradical contribution, because the triplet components are broadened. In the case of tetraradical spectrum **1d**, hyperfine splittings are just barely indicated.

In contrast to the EPR spectra, the ENDOR spectra of the different oxidation steps are well resolved (Figure 1, right). The hyperfine coupling constants (of the galvinoxyl ring protons) can be extracted by means of the ENDOR resonance condition for multispin systems

$$\nu_{ENDOR} = |\nu_n - M_S a^S| \quad (2)$$

where ν_n denotes the free nuclear Larmor frequency (i.e., ν_H = 14.5 MHz) and M_S the magnetic quantum number of the total electron spin.[6,9] As is evident from Figure 1 (right), the ENDOR experiments confirm the presence of the postulated electron spin states, because all expected signals (denoted by arrowheads) can actually be observed. Only the signals that should appear at the free proton Larmor frequency (**1b**,**1d**) cannot be seen for reasons discussed previously,[9,25] i.e., in isotropic fluid solution the EPR transitions connected to the level $M_S = 0$ are pumped equally strongly thus leaving the thermal nuclear spin polarization within this manifold undisturbed. The ENDOR spectra in Figure 1 (right) also reveal contributions from other oxidation steps, since the nature of the EPR spectra of **1a–d** does not allow a sufficiently selective desaturation.

Solid Solution. The zero-field splitting parameters (D, E) of the multispin systems can be determined from EPR spectra recorded in solid solution,[3,26] see Figure 2 (left). The poor resolution of the spectra, probably caused by contributions from different oxidation steps, does not allow an accurate analysis. However, the following D parameters can be estimated from the separation of the outermost fine structure components (z_1, z_2): triplet (**1b**), D = 1.1 mT = 31 MHz [from $^1/_2(B_{z_2} - B_{z_1})$]; quartet (**1c**), D = 0.58 mT = 16 MHz [from $^1/_4(B_{z_2} - B_{z_1})$]. As expected for a molecule with tetrahedral symmetry, the EPR spectrum of quintet species **1d** does not reveal any resolved fine structure ($D = 0$). The D value of **1b** is similar to that of a model compound, namely 4,4′-diphenylmethane bisgalvinoxyl (D = 1.0 mT).[12] On the basis of a simple point dipole model [$|D| = (3\mu_0/8\pi)(g^2\mu_B^2/h)r_{12}^{-3}$],[27] an average distance between the unpaired electrons of r_{12} = 1.37 nm can be estimated, in accordance with model considerations.

Since the degeneracy of the EPR transitions ($|-1,M_I\rangle \leftrightarrow |0,M_I\rangle$ and $|0,M_I\rangle \leftrightarrow |1,M_I\rangle$) is lifted by the zero-field splitting in solid solution,[8] an ENDOR signal of biradical **1b** at the free proton Larmor frequency (line width ≤100 kHz) can now be observed (see Figure 2, top right). Such a signal (line width ca. 140 kHz) is also detected for tetraradical **1d**. It might be taken to indicate a slight deviation from tetrahedral symmetry; note that true T_d symmetry is not achievable for any conformation of **1d**. However, we cannot rule out the alternative possibility that this signal is not associated with the $M_S = 0$ electron spin manifold but due to *tert*-butyl protons with unresolved hyperfine splittings. (This is not a matrix ENDOR line—that might, in principle, also be expected at this position—because it is also detected in perdeuteriotoluene as solvent.)

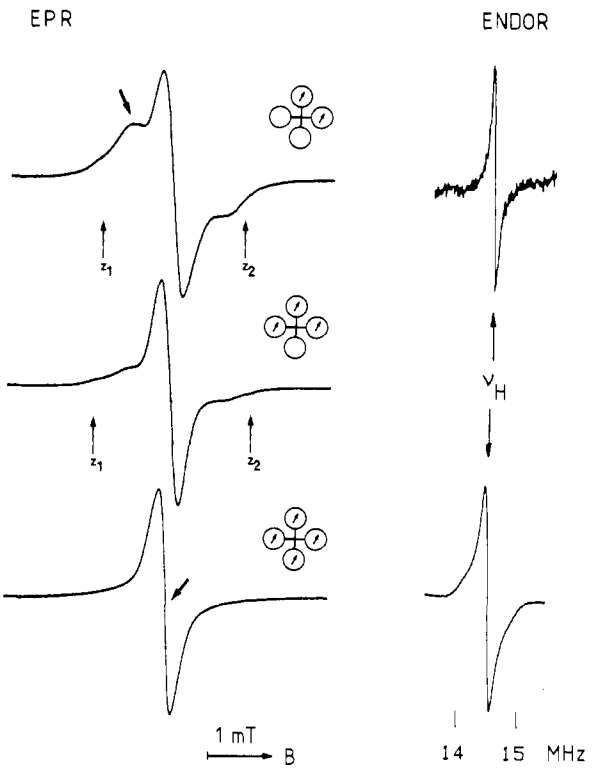

Figure 2. Left: EPR spectra of **1b** (top), **1c** (center), and **1d** (bottom) recorded in glassy toluene (160 K). The turning points (z peaks) and the field settings in the ENDOR experiments are indicated by arrows; zero-field splitting parameters D = 1.1 mT (**1b**) and 0.58 mT (**1c**). Right: central portions (ν_H region) of the ^{1}H ENDOR spectra (**1b** and **1d**).

EPR and ENDOR of 2a–d. EPR and ENDOR spectra of the different paramagnetic species **2a–d** generated from ^{13}C-labeled tetrakisgalvinol **2** are collected in Figure 3. The well-resolved EPR spectrum of monoradical **2a** is dominated by the large ^{13}C hyperfine coupling ($|a_C^d|$ = 0.9927 mT = 27.84 MHz), i.e., it consists of a doublet of quintets. Since the number of contributing ^{13}C nuclei is equal to the number of unpaired electrons in the multispin systems, the ^{13}C hyperfine pattern should reflect the electron spin state quite directly. Thus, triplet state **2b** should exhibit a triplet pattern, quartet state **2c** a quartet pattern, and quintet state **2d** a quintet pattern. Whereas a quintet pattern is actually observed for **2d**, solutions of **2b** and **2c** yield complex EPR spectra for the reasons discussed previously for **1b** and **1c**.

Nevertheless, the ^{13}C hyperfine patterns are beneficial for ENDOR experiments by allowing a selective desaturation of EPR transitions of individual species even in mixtures of radicals in different spin states. Thus, only triplet **2b** and quintet **2d** should exhibit a hyperfine component in the center of the EPR spectrum. The actual field settings are indicated by arrows in Figure 3 (left). The ENDOR spectra depicted in Figure 3 (right) were recorded under conditions optimized for the observation of ^{13}C ENDOR signals,[28] i.e., at higher temperatures and radio-frequency (RF)

(24) Gierke, W.; Harrer, W.; Kirste, B.; Kurreck, H.; Reusch, J. *Z. Naturforsch. B* **1976**, *31*, 965.
(25) van Willigen, H.; Plato, M.; Möbius, K.; Dinse, K. P.; Kurreck, H.; Reusch, J. *Mol. Phys.* **1975**, *30*, 1359.
(26) Wasserman, E.; Snyder, L. C.; Yager, W. A. *J. Chem. Phys.* **1964**, *41*, 1763.
(27) Hirota, N.; Weissman, S. I. *J. Am. Chem. Soc.* **1964**, *86*, 2538.
(28) Kirste, B.; Kurreck, H.; Lubitz, W.; Schubert, K. *J. Am. Chem. Soc.* **1978**, *100*, 2292.

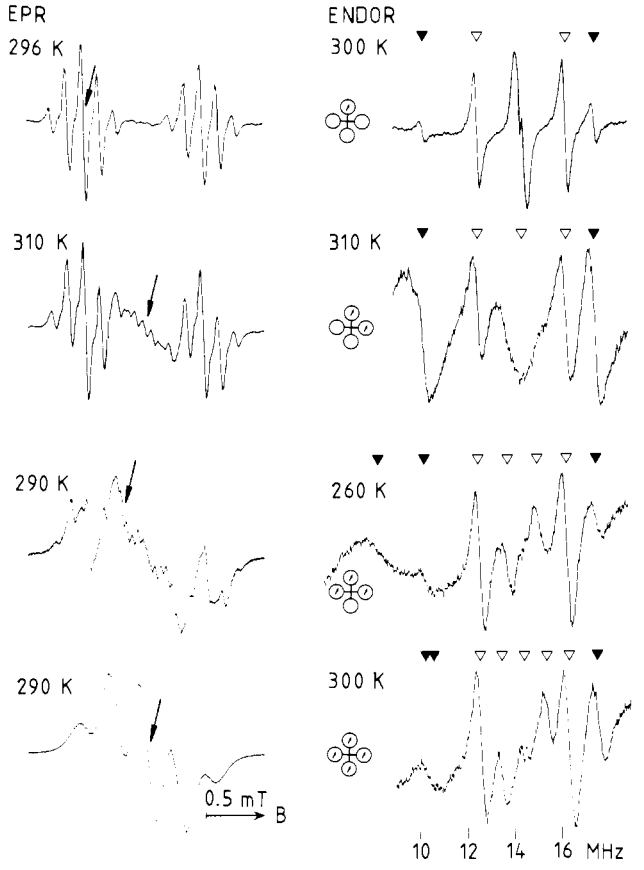

Figure 3. EPR (left) and ENDOR spectra (right) of different paramagnetic oxidation steps of ^{13}C-labeled tetrakisgalvinol **2** in toluene. From top to bottom: monoradical **2a**, biradical **2b**, triradical **2c**, and tetraradical **2d**. The arrows in the EPR spectra indicate the field settings in the ENDOR experiments. The calculated ENDOR signal positions are labeled by open triangles (▽, ^1H ENDOR) and filled triangles (▼, ^{13}C ENDOR), respectively.

Table I. Calculated ^{13}C ENDOR Signal Positions of **2a–d** (in MHz)[a]

2a	2b	2c	2d
17.57 (+1/2)	17.57 (+1)	17.57 (+3/2)	17.57 (+2)
		8.29 (+1/2)	10.61 (+1)
	3.65 (0)		3.65 (0)
		0.99 (−1/2)	3.31 (−1)
10.27 (−1/2)	10.27 (−1)	10.27 (−3/2)	10.27 (−2)

[a] Calculated from eq 1 and 2 with $a_C^d = -27.84$ MHz and $\nu_C = 3.65$ MHz. The respective M_S values (eq 2) are given in parentheses.

power levels than those required for an optimum ^1H ENDOR response (cf. Figure 1). At lower temperatures (e.g., **2a** at 230 K) ^{13}C ENDOR signals cannot be seen.

The calculated signal positions (eq 2) are also indicated in Figure 3 (right) (denoted by open triangles for ^1H ENDOR and by solid triangles for ^{13}C ENDOR). In contrast to ^1H ENDOR, not all the expected ^{13}C ENDOR signals (see Table I) have actually been detected, however. Signals of **2b** and **2d** at the free ^{13}C Larmor frequency ($\nu_C = 3.65$ MHz) cannot be seen for the reasons given above for the failure to observe signals at the free proton Larmor frequency. Signals expected at very low frequencies (**2c**, 1.0 MHz; **2d**, 3.3 MHz; see Table I) could not be detected because of insufficient RF power and, more importantly, severe baseline problems. At 8.3 MHz (**2c**, $M_S = {}^1/_2$) and at 10.6 MHz (**2d**, $M_S = 1$) respectively merely some broad features show up. Thus, only ^{13}C ENDOR signals at 17.6 and at 10.3 MHz are definitely present in each spectrum. As is evident from Table I, the positions of these signals, corresponding to $M_S = \pm S$ (eq 2), are independent of the electron spin state (and of the scalar electron exchange interaction). The hyperfine coupling constants of **2a–d** are collected in Table II. It is noteworthy that the absence

Table II. Hyperfine Coupling Constants of **1a–d** and **2a–d** (in MHz)[a]

compd	spin state	a_H^S	a_C^S
1a, **2a**	doublet	+3.74, +3.62 (220)[b]	−27.84 (300)
1b, **2b**	triplet	+1.87 (290)	−13.92 (310)
1c, **2c**	quartet	+1.24 (250)	−9.31 (300)
1d, **2d**	quintet	+0.92 (210)	−6.97 (300)

[a] ENDOR measurements in toluene, accuracy ±0.02 MHz. Relative signs were determined by general TRIPLE resonance. The temperature (in K) is given in parentheses. For the definition of a^S, see eq 1 and 2. [b] Further coupling constants: +0.58 (phenyl, ortho) and +0.13 MHz (*tert*-butyl).

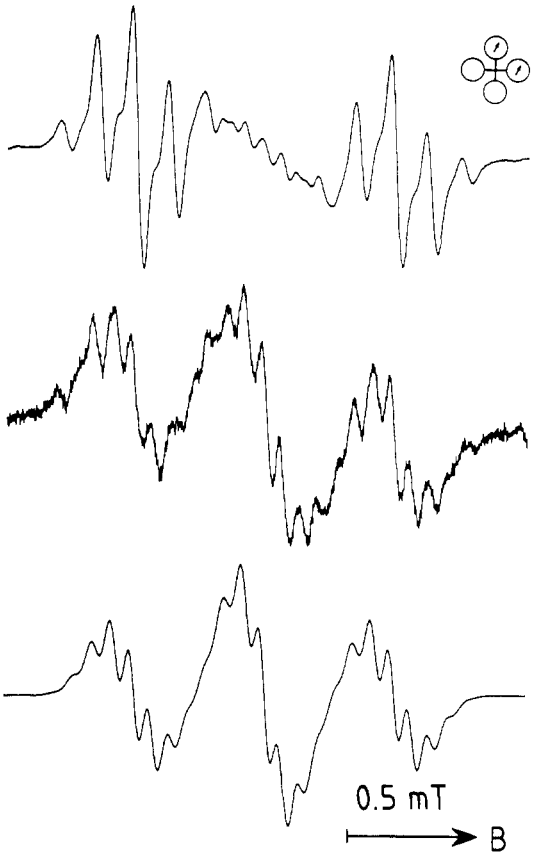

Figure 4. Top: EPR spectrum of **2b** (toluene, 310 K). Center: EPR difference spectrum (see text). Bottom: Computer simulation [a_C = 27.97 MHz (2 × 1 C), a_H = 3.82 MHz (2 × 4 H), J = 660 MHz, line width 0.064 mT (peak-to-peak, Gaussian shape)].

of a sharp ^{13}C ENDOR signal from the $M_S = {}^1/_2$ manifold of triradical **2c** (under various experimental conditions, e.g., temperature and RF power) is in contrast not only to the ^1H ENDOR results for this radical but also to a previous ^{13}C ENDOR study of another triradical, namely ^{13}C-labeled 1,3,5-benzene trisgalvinoxyl.[11] An explanation for the particular behavior of **2c** might be that the scalar electron exchange interaction J, although certainly much larger than the proton hyperfine couplings, is not exceedingly large relative to the ^{13}C hyperfine coupling (vide infra).

More detailed information about the magnitude of the electron exchange interaction should be accessible from a closer inspection of the EPR spectra. Since the experimental spectra of **2b** and **2c** are superposed by considerable contributions from other oxidation steps, the "true" spectra of **2b** and **2c** were reconstructed as difference spectra, i.e., by subtracting the approximate contributions due to the other species. The results of these computer manipulations with experimental spectra are depicted in Figures 4 and 5.

In Figure 4, the original EPR spectrum of biradical **2b** (top) is compared with the respective difference spectrum (center). At first sight, it exhibits just the expected triplet pattern due to hyperfine interaction with two ^{13}C nuclei. The amplitude ratio

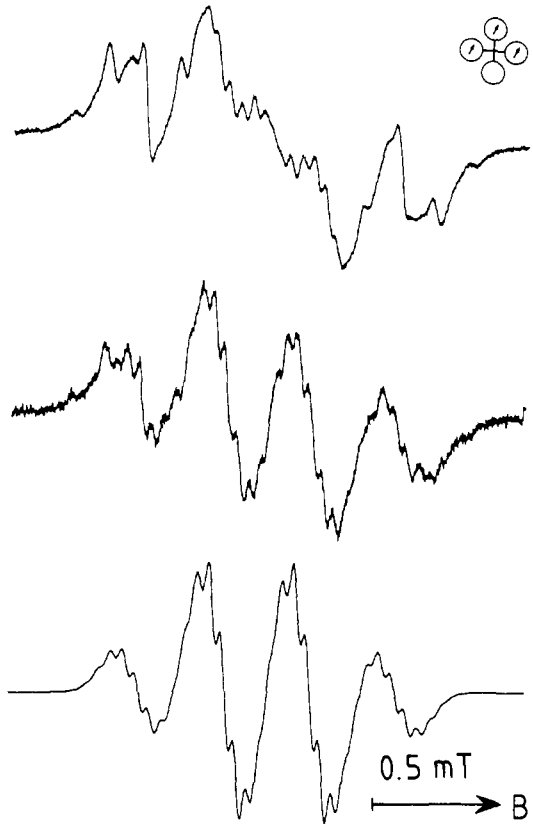

Figure 5. Top: EPR spectrum of **2c** (toluene, 290 K). Center: EPR difference spectrum (see text). Bottom: computer simulation [a_C^q = 9.27 MHz (3 C), a_H^q = 1.29 MHz (12 H), line width 0.049 mT (peak-to-peak, Gaussian shape)].

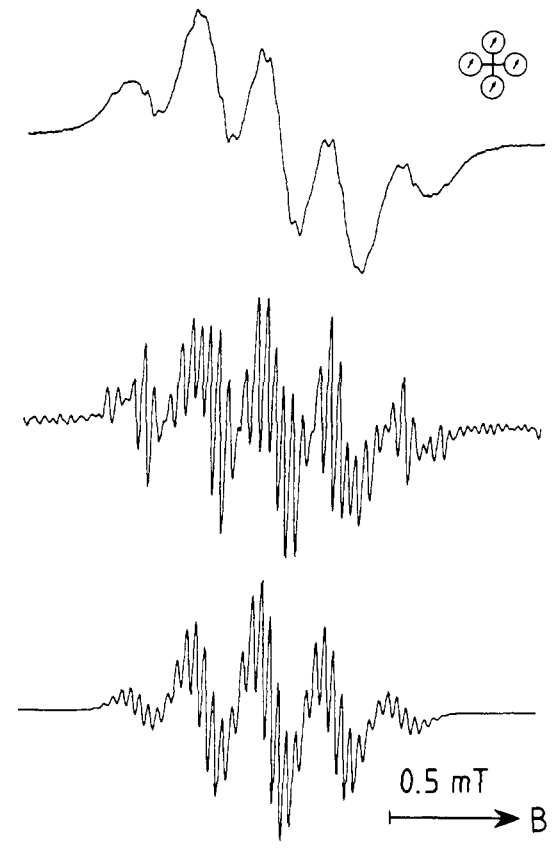

Figure 6. Top: EPR spectrum of **2d** (toluene, 296 K). Center: Resolution-enhanced spectrum (Lorentzian–Gaussian transformation). Bottom: Computer simulation [$a_C^{q\,i}$ = 6.99 MHz (4 C), $a_H^{q\,i}$ = 0.94 MHz (16 H)].

of about 1:1.5:1, however, does not correspond to the binomial ratio of 1:2:1, apparently owing to a somewhat better resolution in the outer components. In Figure 4 (bottom) a computer-simulated spectrum is given, calculated by means of a program for simulating and fitting EPR spectra[29] which was modified to take account of the exchange interaction in biradicals.[30,31] Starting from the limit of strong exchange, decreasing exchange interaction J mainly affects the central ^{13}C hyperfine component, giving rise to a splitting of $(a_C^d)^2/(2J)$ of this component. As computer simulations demonstrate that such a splitting would actually be resolved if $|J| \leq 10|a_C^d|$, the exchange integral must be larger than that. A fairly good agreement with the experimental spectrum is achieved for $|J| = 20|a_C^d|$ (see Figure 4). However, the available experimental data do not allow a very accurate determination of this quantity.

In Figure 5, a comparison of the original EPR spectrum of triradical **2c** (top) and the respective difference spectrum (center) is given. A computer-simulated spectrum that was calculated on the assumption of strong exchange is depicted at the bottom of Figure 5. Again, the amplitude ratio of the experimental difference spectrum of **2c** (about 1:2:2:1) deviates from the binomial ratio (1:3:3:1) because the exchange integral is in fact not exceedingly large. Apart from that restriction, the EPR difference spectrum of **2c** corresponds to that expected for a quartet state, i.e., it does not exhibit any resolved features that may be attributed to the (two) thermally populated doublet states of a triradical ($|J| \ll |k7|$). Diagonalization of the spin Hamiltonian for a triradical (hyperfine interaction with three ^{13}C nuclei, disregarding the protons) demonstrates that the hyperfine components of the doublet states should show up in the wings (with intensities 0.3:0.5:0:0:0.5:0.3). Thus, the total spectrum should exhibit a binomial sextet pattern, which is clearly not in agreement with experiment. Apparently the doublet components are much broader than the quartet components.

The EPR spectrum of tetraradical **2d** is shown again in Figure 6 (top). Apart from a broad underlying feature, it is in fair agreement with a computer simulation for a quintet state ($|J| \gg |a_C^d|$), but definite conclusions about the magnitude of the exchange integral J cannot be drawn. Resolved hyperfine components of thermally populated triplet states (with calculated intensities of 0.8:1.8:0:4.4:0:1.8:0.8) cannot be seen. Obviously proton hyperfine splittings are merely indicated in the EPR spectrum of **2d**. They can be resolved by means of resolution enhancement techniques (Lorentzian–Gaussian transformation),[32] see Figure 6 (center). A computer simulation calculated for the limit of strong exchange is given at the bottom of Figure 6.

In order to examine the effects of the exchange interaction on the ENDOR spectra of the multispin systems **2b–d**, the ^{13}C signal positions were calculated by numerical diagonalization of the Hamiltonian matrix of the respective spin system, assuming $|J| = 20|a_C^d|$. Relaxation effects or particularities of the ENDOR method[33] were not taken into account. As has been suggested above, ^{13}C ENDOR signals at 10.3 and 17.6 MHz from NMR transitions within the manifolds $M_S = \pm S$ are indeed independent of the electron spin state and the magnitude of the exchange interaction. In accordance with a previous theoretical study,[34] the signal of biradical **2b** expected at the free ^{13}C Larmor frequency should be split into a doublet with a spacing of $(a_C^d)^2/(2J) \approx 0.70$ MHz. For the signals of triradical **2c** arising from the manifolds $M_S = \pm^1/_2$ (cf. Table I), triplet splittings with spacings of 0.21 MHz are calculated. Moreover, the calculation predicts

(29) Kirste, B. *J. Magn. Reson.* **1987**, *73*, 213.
(30) Reitz, D. C.; Weissman, S. I. *J. Chem. Phys.* **1960**, *33*, 700.
(31) Kirste, B.; Krüger, A.; Kurreck, H. *J. Am. Chem. Soc.* **1982**, *104*, 3850.
(32) Roth, K.; Kirste, B. *J. Magn. Reson.* **1985**, *63*, 360.
(33) Plato, M.; Lubitz, W.; Möbius, K. *J. Phys. Chem.* **1981**, *85*, 1202.
(34) Brauer, H.-D.; Stieger, H.; Hyde, J. S.; Kispert, L. D.; Luckhurst, G. R. *Mol. Phys.* **1969**, *17*, 457.
(35) Tousley, N. E.; Gomberg, M. *J. Am. Chem. Soc.* **1904**, *26*, 1516.

a pair of signals at 19.5 and 26.9 MHz due to the doublet states of **2c**. In an experimental reinvestigation (with off-center field settings) these ENDOR signals could not be observed, however. The calculation for the tetraradical **2d** yields the following result: signals at 10.25 and 17.59 MHz ($M_S = \pm 2$, see Table I), a doublet around 10.63 MHz (10.54 and 10.72 MHz, $M_S = 1$), a series of signals between 2.8 and 4.5 MHz (from $M_S = 0, -1$), and signals at 17.2 and 24.5 MHz (from the triplet states; not observed). In summary, these theoretical results are in accordance with experimental findings, i.e., sharp ^{13}C ENDOR signals are expected only from the manifolds $M_S = \pm S$, otherwise split (or broadened) signals are predicted. The failure to observe resolved EPR or ENDOR signals due to lower spin states of **2c** or **2d** may be attributed to line broadening caused by proton hyperfine interactions or relaxation effects.

Conclusions

Concluding we can state that selective oxidation of a tetrakisgalvinol allowed the generation and investigation of the respective mono-, bi-, tri-, and tetraradical. We have established the presence of a quintet state in the approximately tetrahedral tetrakisgalvinoxyl by means of EPR and ENDOR spectroscopy. Whereas the observed ^1H ENDOR spectra are in full agreement with expectation for a quintet-state tetraradical, and likewise with a quartet-state triradical and a triplet-state biradical, ^{13}C ENDOR spectroscopy proved to be a more sensitive probe of the magnitude of the scalar electron exchange interaction J. Computer simulations of EPR difference spectra yielded an estimate of $J \approx 600$ MHz, determined for the biradical. It must be pointed out that ^{13}C labeling was a prerequisite for these studies.

Experimental Section

Preparation of Compounds. Since experimental procedures for the preparation of ^{13}C-labeled tetrakisgalvinol **2** have been reported previously,[13] these will not be repeated here. In the following, procedures pertaining to Scheme I are given.

Tetrakis(4-methylphenyl)methane (7). Method A. To 75 g (234 mmol) of tris(4-methylphenyl)chloromethane[35] in 1.2 L of absolute toluene a solution of 4-methylphenylmagnesium bromide [from 80.2 g (469 mmol) of 4-bromotoluene and 23 g of Mg in 300 mL of ether] was added with stirring under argon. After 48 h, the mixture was hydrolyzed with ice and dilute HCl. The organic layer was separated and washed with water, and the solvent was removed under vacuum. Byproducts were removed by steam distillation. Recrystallization from ether/methanol yielded 10.4 g (11.8%) of **7**; mp 254.5–255.5 °C. Mass spectrum (80 eV, 200 °C), m/z 376 (M^+, 48%), 361 ($M^+ - Me$, 15%), 285 ($M^+ - Ph - Me$, 100%). ^1H NMR ($CDCl_3$, 250 MHz) δ 7.11 (m, 16 H, aryl), 2.34 (s, 12 H, Me). **Method B.** Methyllithium, from 0.68 g (98 mmol) of Li and 3 mL (48 mmol) of iodomethane in 15 mL of ether, was added to a solution of 2 g (3.14 mmol) of tetrakis(4-bromophenyl)methane[13] in 80 mL of absolute tetrahydrofuran at −50 °C under argon. The temperature was slowly raised to −5 °C and the mixture was stirred for 40 h. Then solvents were removed under vacuum, and the residue was taken up in dichloromethane, washed with water, and dried over Na_2SO_4. After removal of solvent, 1.25 g of crude material was obtained. Yield 0.55 g (46.5%, determined by HPLC).

Tetrakis(4-cyanophenyl)methane (5). A mixture of 5.94 g (9.34 mmol) of tetrakis(4-bromophenyl)methane,[13] 4.68 g (71.9 mmol) of potassium cyanide, 0.72 g (4.34 mmol) of potassium iodide, 1 mg (18 μmol) of potassium hydroxide, 0.12 g (0.53 mmol) of palladium(II) acetate, and 54 mL of anhydrous hexamethylphosphortriamide was heated under argon for 19 h at 95 °C (oil bath) with stirring. (The mixture turns black; if it decolorizes, more palladium(II) acetate must be added.) Then the light brown suspension was evaporated to dryness under vacuum (1 hPa, 90–150 °C). The residue was taken up in dichloromethane, washed with water, dried over Na_2SO_4, and filtered through a short column with silica gel/dichloromethane. Purification by recrystallization from chloroform/methanol gave a yield of 3.89 g (99.0%, determined by HPLC); mp 311–312 °C. Anal. Calcd for $C_{29}H_{16}N_4$: C, 82.84; H, 3.84; N, 13.33. Found: C, 82.92; H, 3.94; N, 13.39. Mass spectrum (80 eV, 150 °C), m/z 420 (M^+, 59%), 318 ($M^+ - Ph - CN$, 100%), 216 ($M^+ - 2Ph - 2CN$, 68%). ^1H NMR (CD_2Cl_2, 250 MHz) δ 7.62 (m, AA′BB′, 8 H), 7.29 (m, AA′BB′, 8 H).

Tetraphenylmethane-4,4′,4″,4‴-tetracarboxylic Acid Tetramethyl Ester (3, R = Me). Method A, from 7. Chromium trioxide (100 mmol) and 1.5 mL of concentrated sulfuric acid were added slowly with cooling and stirring to 100 mL of acetic acid and 40 mL of acetic anhydride. At 10 °C, 2 g (5.32 mmol) of powdered **7** were added. After being stirred for 30 min, the mixture was poured into ice water and precipitated **4** was collected by suction filtration. Crude **4** (0.95 g) was purified by dissolving in dilute NaOH and precipitating with dilute HCl (pH 2), washed with water, and dried under vacuum at 150 °C. A suspension of **4** in ether/methanol (9:1) was esterified with diazomethane at room temperature. A part of the product (1.02 g) was purified by HPLC (7C18MN, 8 × 250 mm, 90% methanol, 12 MPa), yielding 30% of benzophenone-4,4′-dicarboxylic acid dimethyl ester (mp 229.5–230 °C; mass spectrum, m/z 298 (M^+)) and 44% of **3** (15.3% relative to **7**); mp 211.5–212.5 °C. Anal. Calcd for $C_{33}H_{28}O_8$: C, 71.73; H, 5.11. Found: C, 71.87; H, 5.15. Mass spectrum (80 eV, 220 °C), m/z 552 (M^+, 64%), 521 ($M^+ - OMe$, 33%), 493 ($M^+ - COOMe$, 26%), 417 ($M^+ - Ph - COOMe$, 100%). ^1H NMR (CD_2Cl_2, 250 MHz) δ 7.88 (m, AA′BB′, 8 H), 7.29 (m, AA′BB′, 8 H), 3.85 (s, 12 H, Me). **Method B, from 5.** **5** (0.42 g, 1 mmol) and 1 g (17.8 mmol) of potassium hydroxide in 10 mL of ethylene glycol were heated under reflux for 19 h with stirring. After dilution with water (100 mL), **4** was precipitated with dilute HCl (pH 2) and purified and esterified as described above (method A). Crude yield of **3**: 0.55 g (purity 99.4% determined by HPLC, i.e., 98.9% yield relative to **5**). The mass spectrum (11 eV, 150 °C) of the ^{13}C-labeled compound, $C_{29}{}^{13}C_4H_{28}O_8$, is in accordance with the expected degree of labeling (99% enrichment, 96% [$^{13}C_4$]) within experimental accuracy, m/z 555 (0.9% found/2.8% calcd), 556 (M^+, 72.9%/68.8%), 557 (22.1%/22.8%), 558 (4.1%/4.8%).

Tetrakis[4-[(3,5-di-*tert*-butyl-4-hydroxyphenyl)(3,5-di-*tert*-butyl-4-oxocyclohexa-2,5-dienylidene)methyl]phenyl]methane (1). To a solution of 15.92 g (44.5 mmol) of (4-bromo-2,6-di-*tert*-butylphenoxy)trimethylsilane in absolute tetrahydrofuran (200 mL) 55.7 mL (88.1 mmol) of a solution of *tert*-butyllithium in *n*-pentane (1.6 M) was added at −70 °C under argon within 45 min, after 40 min followed by a cooled solution of 1 g (1.81 mmol) of **3** in anhydrous tetrahydrofuran (70 mL). Within 1.5 h the mixture was allowed to warm up to −30 °C, and then water (several milliliters) was added. Cleavage of the trimethylsilyl groups was achieved with stirring for 12 h at room temperature, and then the dark blue solution was acidified with dilute HCl. After dilution with ether, the orange solution was washed with water, the organic layer was separated, and solvents were removed under vacuum. Purification was done by flash chromatography[36] (silica gel 40–63 μm [Merck 9385], 80 × 80 mm, dichloromethane); crude yield 3.59 g (purity 94% determined by HPLC, i.e., 93.2% yield relative to **3**). A part of the product was purified by HPLC (7 μm Polygosil 60 KN, 32 × 250 mm, dichloromethane); mp >360 °C. Anal. Calcd for $C_{141}H_{180}O_8$: C, 84.55; H, 9.06. Found: C, 84.20; H, 8.93. Mass spectrum (80 eV, 450 °C), m/z 2000 (M^+), 2001 (100%); peaks in the region from $M^+ - 4$ to $M^+ + 4$ arise from loss or addition of hydrogen. ^1H NMR (CD_2Cl_2, 250 MHz) δ 7.32 (m, AA′BB′, 8 H), 7.29 (d, J = 1.6 Hz, 4 H, quinoid), 7.20 (m, AA′BB′, 8 H), 7.14 (d, J = 1.6 Hz, 4 H, quinoid), 7.06 (s, 8 H, phenolic rings), 5.55 (s, 4 H, Ar–OH; D_2O exchange), 1.38 (s, 72 H, *t*-Bu), 1.26 (s, 36 H, *t*-Bu), 1.18 (s, 36 H, *t*-Bu). ^{13}C NMR ($CDCl_3$, 62.9 MHz) δ 186.01 (C=O), 156.91 (Cq, labeled position in **2**), 155.44 (C–OH), 147.11 (Cq), 146.71 (Cq), 146.66 (Cq), 139.95 (Cq), 135.39 (Cq), 132.21 (CH), 131.61 (Cq), 131.34 (CH), 130.39 (CH), 129.74 (CH), 128.81 (Cq), 64.87 (Cq, central), 35.33 (Cq), 35.25 (Cq), 34.40 (Cq), 30.27 (CH_3), 29.68 (CH_3), 29.43 (CH_3). The mass spectrum (30 eV, 300 °C) of ^{13}C-labeled compound **2** is in accordance with the expected degree of labeling (96% [$^{13}C_4$]), m/z 2005 (100%).

Generation of Radicals. Tetraradicals **1d** and **2d** were generated by oxidation of solutions of the respective tetrakisgalvinols (**1** or **2**) in toluene (Uvasol, Merck) with aqueous $K_3[Fe(CN)_6]$/KOH. The organic layer was transferred to an EPR/ENDOR sample tube and carefully deoxygenated by flushing with purified N_2. Solutions of the bi- and triradicals were prepared by synproportionation, i.e., by mixing solutions of **1d** and **1** (or **2d** and **2**) in the appropriate ratio (1:1 or 3:1, respectively), assuming essentially statistical behavior of the redox equilibria. For the generation of monoradicals (**1a**, **2a**), a large excess of a solution of **1** (**2**) was added to **1d** (**2d**).

Instrumentation. EPR, ENDOR, and TRIPLE spectra were recorded on a Bruker ER 220D EPR spectrometer equipped with a Bruker cavity (ER 200ENB) and laboratory-built NMR facilities described elsewhere.[6,7] The spectrometer was interfaced to a minicomputer (HP 1000/A600) used for controlling the scan oscillator and the RF (radio frequency) power (which was kept constant over the frequency range) in ENDOR experiments in addition to data acquisition and handling and storage of the spectra. EPR spectra were accumulated by using a Nicolet 1170 signal averager employing 1–4K data points and afterwards transferred to the minicomputer. ENDOR spectra of ^{13}C-labeled mul-

(36) Still, W. C.; Kahn, M.; Mitra, A. *J. Org. Chem.* **1978**, *43*, 2923.

tispin systems were typically obtained with microwave power levels of 20 mW (monoradical **2a**), 200 mW (biradical **2b**), 100 mW (triradical **2c**), or 40 mW (tetraradical **2d**), RF power levels of 200-400 W (corresponding to $B_{RF} \approx 0.6$-0.8 mT in the rotating frame), and frequency modulation amplitudes of 60-100 kHz; 100 to 200 spectra were accumulated, scan time 30 s, time constant 40 ms, 1000 data points. For comparison, the ENDOR spectrum of **1a** was recorded with an RF power of 40 W, FM amplitude of 30 kHz, and time constant 12.5 ms. NMR spectra were recorded with a Bruker AC 250 spectrometer. Mass spectra (EI) were obtained on a Varian MAT 711 double-focusing instrument.

Acknowledgment. B. K. and H. K. gratefully acknowledge financial support by the Fonds der Chemischen Industrie and the Deutsche Forschungsgemeinschaft (Normalverfahren, H. K.).

Registry No. 1, 117679-70-6; **1a**, 117679-71-7; **1b**, 117686-95-0; **1c**, 117686-96-1; **1d**, 117679-72-8; **3** (R = Me), 105309-62-4; **5**, 105309-60-2; **7**, 117679-69-3; ^{13}C, 14762-74-4; tris(4-methylphenyl)chloromethane, 117679-68-2; 4-methylphenylmagnesium bromide, 4294-57-9; tetrakis(4-bromophenyl)methane, 105309-59-9; (4-bromo-2,6-di-*tert*-butylphenoxy)trimethylsilane, 27329-74-4.

^{14}N Quadrupole Double Resonance in Some Substituted Hydroxamic Acids

Wang Ruiqin,[†] Yu Xiaolan,[†] Feng Zhenye,[†] Mian M. I. Haq,[‡] Muhammed M. P. Khurshid,[‡] Timothy J. Rayner,[‡] John A. S. Smith,*[,‡] and Michael H. Palmer[§]

Contribution from the Departments of Chemistry and Electronics, Zhongshan University, Guangzhou, China, Department of Chemistry, King's College, Strand, London WC2R 2LS, U.K., and Chemistry Department, University of Edinburgh, West Mains Road, Edinburgh EH9 3JJ, U.K. *Received April 20, 1988*

Abstract: ^{14}N quadrupole coupling constants and asymmetry parameters have been measured in a number of hydroxamic acids by double-resonance field-cycling techniques based on either irradiation in zero magnetic field or cross relaxation. The compounds all display high asymmetry parameters. Those in which this quantity is greater than 0.9 show remarkable line shapes for the two lower ^{14}N frequencies (ν_y, ν_z) in their irradiation spectra. They are explained in terms of a thermal-mixing mechanism, which generates polarization of the ^1H dipolar levels when these nearly degenerate frequencies are strongly irradiated in zero field, and then subsequently modified by level crossing when the sample is returned to high field to measure the remaining ^1H signal. Ab initio SCF-MO calculations of the ^{14}N quadrupole tensor in a group of molecules at the orientation found in crystals of acetohydroxamic acid hemihydrate and oxalodihydroxamic acid are in reasonable agreement with experiment and predict that in all the hydroxamic acids studied the maximum principal component is negative and closely parallel to the direction of the $2p_\pi$ orbital.

It has been known for many years[1] that hydroxamic acids, RCONHOH, can exist in two tautomeric forms (**1** and **2**).

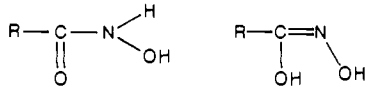

1 **2**

The equilibrium has been much studied in solution by infrared spectroscopy,[2-6] dipole moment measurements,[7-9] and ^1H, ^{13}C, and ^{17}O magnetic resonance spectroscopy,[10-14] but, apart from some infrared studies and X-ray crystal structure analyses of acetohydroxamic acid hemihydrate,[15] salicylhydroxamic acid,[16] malonohydroxamic acid,[17] nicotinohydroxamic acid,[17] and oxalodihydroxamic acid,[18] few other studies have been made of the structure of these molecules in the solid state. The purpose of this article is 3-fold: to show, first, that the two forms (**1** and **2**) can be distinguished in solids by the techniques of ^{14}N quadrupole double-resonance spectroscopy; second, that, in structure **1**, the high asymmetry parameter and short spin-lattice relaxation time in some of these compounds at room temperature lead to unusual line shapes in double-resonance irradiation experiments caused by coupling of the nearly degenerate low-frequency ^{14}N transitions ν_z, ν_y to the ^1H dipolar levels in zero magnetic field; third, that the observed quadrupole parameters can be reproduced quite closely by ab initio SCF-MO calculations and reasonably reliable directions inferred for the principal components of the ^{14}N quadrupole coupling tensor.

Experimental Section

Nine hydroxamic acids, RCONHOH, or related compounds **3**-**11**, were prepared for the purpose of this investigation,[19] namely, malono-

[†] Zhongshan University.
[‡] King's College.
[§] University of Edinburgh.

(1) Sidgwick, N. V. *Organic Chemistry of Nitrogen*; Taylor, T. W. J., Baker, W., Eds.; Clarendon: Oxford, 1942; Chapter VI.
(2) Mathis, F. D. *C. R. Hebd. Seances Acad. Sci.* **1951**, *232*, 505-507.
(3) Hadži, D.; Prevoršek, D. *Spectrochim. Acta* **1957**, *10*, 38-51.
(4) Horák, M.; Exner, O. *Chem. Listy* **1958**, *52*, 1451-1459.
(5) Exner, O.; Kakac, B. *Collect. Czech. Chem. Commun.* **1963**, *28*, 1656-1663.
(6) Exner, O. *Collect. Czech. Chem. Commun.* **1964**, *29*, 1337-1343.
(7) Exner, O.; Jehlička, V.; Reiser, A. *Collect. Czech. Chem. Commun.* **1959**, *24*, 3207-3221.
(8) Exner, O.; Jehlička, V. *Collect. Czech. Chem. Commun.* **1965**, *30*, 639-651.
(9) Exner, O. *Collect. Czech. Chem. Commun.* **1965**, *30*, 652-663.
(10) Mizukami, S.; Nagata, K. *Chem. Pharm. Bull.* **1966**, *14*, 1249-1255, 1263-1272.
(11) Price, B. J.; Sutherland, I. O. *Chem. Commun.* **1967**, 1070-1071.
(12) Walter, W.; Schaumann, E. *Ann. Chim. (Paris)* **1971**, *747*, 191-193.
(13) Kalinin, V. N.; Franchuk, I. F. *Zh. Prikl. Spektrosk.* **1972**, *16*, 692-698.
(14) Lipczyñska-Kochany, E.; Iwamura, H. *J. Org. Chem.* **1982**, *47*, 5277-5282.
(15) Bracher, B. H.; Small, R. W. H. *Acta Crystallogr.* **1970**, *B26*, 1705-1709.
(16) Larsen, I. K. *Acta Crystallogr.* **1978**, *B34*, 962-964.
(17) Ruiqin, W. to be published in *Jiegou Huaxue*.
(18) Lowe-Ma, C. K.; Decker, D. L. *Acta Crystallogr.* **1986**, *C42*, 1648-1649.

0002-7863/89/1511-0114$01.50/0